RSC Advances

PAPER

View Article Online
View Journal | View Issue

Cite this: *RSC Adv.*, 2026, **16**, 20946

Aging and degradation behaviour of poly(lactic acid) composites in alcoholic and acidic food simulants

Andrei Moldovan,[a] Ionut Sarosi,[a] Violeta Popescu,[a] Stanca Cuc, *[b] Codruta Sarosi,[b] Cezara Zagrean-Tuza,[c] Radu Silaghi-Dumitrescu, [c] Ovidiu Nemes*[ad] and Ancuta-Elena Tiuc[a]

The increasing demand for sustainable, high-performance materials in food packaging highlights the need to understand how bio-based additives and metallic nanofillers influence the stability and degradation behavior of polylactic acid (PLA) composites under food-contact conditions. In this study, PLA-based composites containing grape pomace and silver or copper nanoparticles were developed and evaluated in terms of physico-chemical stability, thermal behavior, and degradation mechanisms. Two commercial PLA grades (PLA1 and PLA2) were blended with Proviplast 2624 plasticizer and doped with grape pomace powder or Ag-PEG/Cu-PEG nanofillers. Nine composite formulations were prepared by melt processing and immersed for six months in three food simulants (10% ethanol, 3% acetic acid, and 20% ethanol) to investigate mass variation, Vickers hardness, surface morphology, and chemical and thermal changes. Scanning electron microscopy (SEM), electron paramagnetic resonance (EPR), Fourier transform infrared spectroscopy (FTIR), and differential scanning calorimetry (DSC) were used to correlate morphological, chemical, and structural modifications occurring during exposure. The results showed that both composite formulation and simulant type significantly affected the structural, mechanical, and degradation behavior of the materials. Grape pomace–reinforced samples exhibited increased Vickers hardness after immersion, particularly in ethanolic media, attributed to the rigid structure of the filler and its stabilizing effect on the polymer matrix. Composites containing Ag-PEG and Cu-PEG nanofillers showed improved nanoparticle dispersion and partial stabilization of the PLA matrix, with enhanced performance at 8% nanoparticle loading. However, prolonged exposure to simulants resulted in polymer degradation characterized by mass variation, surface damage, and free-radical formation detectable by EPR. FTIR and DSC analyses indicated structural and thermal changes consistent with hydrolysis-induced chain scission, while acetic acid proved to be the most aggressive medium, accelerating hydrolytic degradation and structural fragmentation.

Received 16th February 2026
Accepted 31st March 2026

DOI: 10.1039/d6ra01374k

rsc.li/rsc-advances

Introduction

Polylactic acid (PLA) is one of the most widely used polymers in the food packaging industry due to its biodegradability, transparency, and suitability for short-term applications such as plates, cups, lids, and drinking straws.[1–3] Despite its renewable origin and compostability, PLA exhibits several limitations that restrict its broader use in food packaging, including relatively poor water–vapor barrier properties, limited mechanical and thermal performance, low ductility, and lower thermal stability compared with conventional petroleum-based polymers.[4,5] These shortcomings have stimulated increasing research interest in the development of PLA-based composites containing functional fillers and additives in order to improve their overall performance and long-term stability.[6] To address these shortcomings, various strategies have been explored, including polymer blending, the incorporation of fillers, and the use of plasticizers to tailor the properties of PLA for specific applications.[7–9]

Among these approaches, plasticizers such as thermoplastic starch (TPS), polyethylene glycol (PEG), poly(ε-caprolactone), and poly(vinyl acetate) have been widely employed to improve flexibility, impact resistance, and elongation at break of PLA-based materials.[10–17] However, these modifications alone are often insufficient to fully over-come the intrinsic limitations of

[a]*Technical University of Cluj-Napoca, Faculty of Materials and Environmental Engineering, 103-105 Muncii Ave, Cluj-Napoca, Romania. E-mail: ovidiu.nemes@sim.utcluj.ro*

[b]*Babeș-Bolyai University, Raluca Ripan Institute for Research in Chemistry, 30 Fantanele Street, 400294 Cluj-Napoca, Romania. E-mail: stanca.boboia@ubbcluj.ro*

[c]*Faculty of Chemistry and Chemical Engineering, Babeș-Bolyai University, 11 Arany János Street, 400028 Cluj-Napoca, Romania*

[d]*National Institute for Research and Development in Environmental Protection, 294 Splaiul Independenței Blv., District 6, 060031 Bucharest, Romania*

PLA, particularly in applications requiring enhanced stability and durability under different environmental conditions relevant to packaging systems.

Beyond purely mechanical improvements, increasing attention has been directed toward incorporating bio-based additives and inorganic fillers into biodegradable polymers to modify their physicochemical behaviour and degradation characteristics. In this context, plant-based by-products such as grape pomace (seeds, stems, and skins), which are rich in phenolic compounds, have attracted significant attention as sustainable additives that may influence the structural and chemical behaviour of polymer matrices.[18,19]

Biodegradable nanocomposites based on synthetic polymer matrices combined with inorganic nanoparticles, such as polyurethane systems reinforced with ZnO, have also been investigated for their ability to modify material properties and degradation behaviour. For example, a polyurethane–chitosan nanocomposite containing ZnO nanoparticles exhibited up to 86% weight loss after 28 days of soil burial.[20] However, such systems rely on synthetic matrices and do not incorporate plant-based macromolecular additives.

Similarly, metallic nanoparticles—including silver (Ag), copper (Cu), and zinc oxide (ZnO)—are widely studied as functional additives in polymeric materials due to their well-known antimicrobial properties and their ability to modify physicochemical characteristics of polymer matrices.[21–30] When incorporated into biodegradable polymers, these particles may influence structural stability, degradation behaviour, and interactions with surrounding media.

Therefore, the aim of this study is to develop and characterize two types of PLA-based nanocomposites: (i) materials incorporating grape pomace and (ii) materials containing metallic antimicrobial additives (Ag-PEG or Cu-PEG), and to investigate how each additive type independently affects the physicochemical properties, stability, and degradation behaviour of PLA-based materials under conditions simulating food-contact environments. Rather than examining antimicrobial performance in food systems, this work compares their respective roles as modifiers of PLA matrices. Through this approach, the study aims to improve the understanding of how different additives influence the long-term behaviour of PLA composites and to support the development of more robust biodegradable materials for potential packaging applications.

Experimental

Materials and methods

Two types of base PLA polymers were used: PLA1 supplied by Nature Works LLC under the Ingeo 2003D® brand (Tokyo, Japan)[31] and PLA2, Luminy LX975 (Gorinchem, The Netherlands). Both materials exhibit comparable bulk densities ($\sim$1.24 g cm^{-3}) and high optical transparency under identical processing conditions; however, they differ slightly in tensile strength (53 MPa and 40 MPa, respectively) and melting temperature (145 °C and 130 °C, respectively).

PLA 1 (Ingeo™ 2003D) has a number-average molecular weight (Mn) of approximately 100 422 g mol^{-1}, a weight-average molecular weight (M_w) of about 180 477 g mol^{-1}, and a PDI of approximately 1.79. These values indicate a semi-crystalline material typically used in packaging applications and a D-lactide content of around 4.3%, which affects its crystallinity and mechanical properties. PLA1as used for grape pomace samples due to its higher strength and viscosity, which promote uniform dispersion and compatibility of the natural particles.

For PLA2 (Luminy® LX975), gel permeation chromatography measurements indicate a number average molecular weight (Mn) of approximately 99 400 g mol^{-1} and a weight average molecular weight (M_w) of approximately 152 500 g mol^{-1}, corresponding to a polydispersity index (M_w/M_n) of $\sim$1.53, which reflects the molecular weight distribution of this commercial PLA grade. PLA 2 was selected for copper nanoparticle samples because its lower viscosity and melting point facilitate efficient nanoparticle dispersion while minimizing polymer thermal degradation.

Proviplast 2624 (Proviron, Hangzhou, China) was used as a plasticizer.[32]

As additives, grape pomace powder as well as Cu and Ag clusters were incorporated. These were obtained in the Polymer Composites Department of the Raluca Ripan Institute for Research in Chemistry at Babeș-Bolyai University, Cluj-Napoca.[33] Grape pomace powder was produced from residues resulting from wine processing (seeds, stems, and skins). The material was dried in a Memmert oven for 8 hours at 60 °C. Stems were separated from the remaining by-products, which were subsequently milled using a PM100 Retsch ball mill until fibrous particles below 100 μm were obtained.

Cu clusters were synthesized by mixing $CuSO_4$ powder with PEG 600 at a 15 : 75 weight ratio for 1 hour. A 10% ascorbic acid solution was then added, and the mixture was stirred for an additional hour to ensure complete homogenization. The resulting gel was stored at 4 °C for 24 hours and subsequently kept at room temperature.

The synthesis started with 4 g of silver nitrate ($AgNO_3$), which was mixed in 50 cm^3 of polyethylene glycol (PEG) at 23 °C for 1 hour using a magnetic stirrer equipped with a temperature-controlled heating system. The temperature was then gradually raised to 90 °C and maintained under continuous stirring for 3 hours.[34] All chemicals used were of analytical-grade purity.

Preparation of the composite mixtures

Nine composite formulations were prepared and investigated as shown in Table 1. The composite mixtures were melt processed in a Brabender plastograph at 180 °C, using a rotor speed of 60 rpm, for 15 minutes.

The visual aspects of the prepared films of several composites compared with plasticized PLA are shown in Fig. 1.

Investigation methodes

Electron paramagnetic resonance (EPR). Electron paramagnetic resonance (EPR) measurements were performed to detect paramagnetic species and radical formation in the polymer composites. This analysis provides insight into

Table 1 Composition of the investigated formulations

Cod%	PLA1	PLA2	Proviplast 2624	Ag-PEG	Cu-PEG	Grape pomace
C1	100					
C2		100				
R1	84.5		15			0.5
R2	84		15			1
R3	83.5		15			1.5
R4		83	15	2		
R5		80	15	5		
R6		77	15	8		
R7		83	15		2	
R8		80	15		5	
R9		77	15		8	

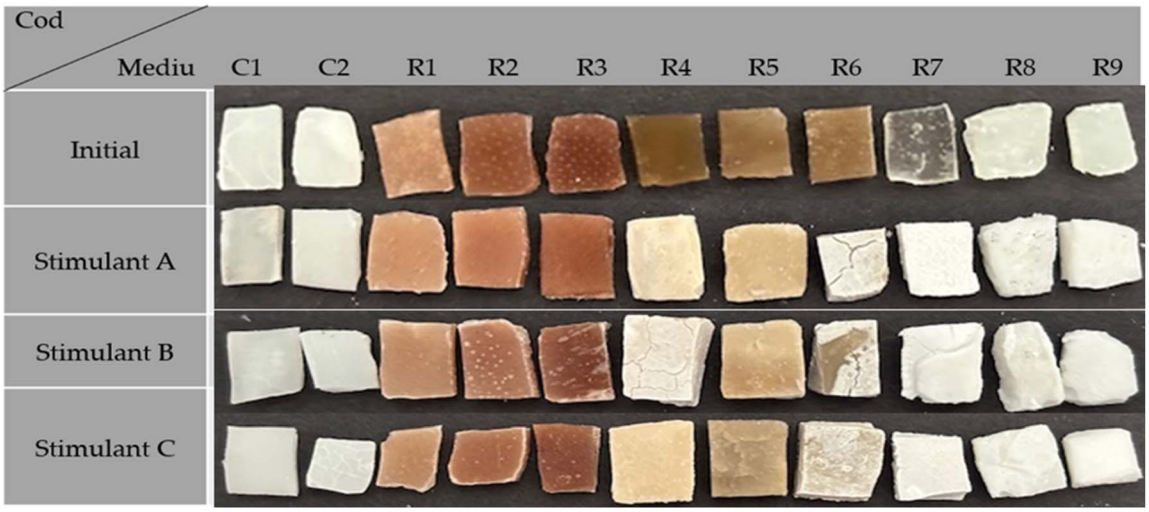

Fig. 1 Optical images before and after 6 months of immersion in the simulants.

oxidative stability and the chemical state of incorporated metal nanoparticles.

Electron paramagnetic resonance (EPR) spectra were recorded using a Bruker X-band ELEXSYS E580 spectrometer in continuous-wave mode at room temperature. A volume of 50 μL of each polylactic formulation was pipetted into a glass capillary and analyzed over a 5000 gauss range (centre field 2505 gauss), with a sweep time of 40 s, a modulation amplitude of 3 gauss, and 10 scans. The antioxidant activity was evaluated using the ABTS radical cation decolorization assay, in which the $ABTS^{\bullet+}$ radical is generated by oxidation with potassium persulfate and the decrease in absorbance at 734 nm is monitored after reaction with antioxidant compounds.[48]

Adsorption under long-term storage conditions for 6 months (≈182.5 days or 1.58 × 10^7 s) at ambient temperature. Mass change measurements were performed to assess the thermal and chemical stability of the polymer composite, providing insight into its suitability for food packaging applications and predicting its behavior during storage and processing.

The amount of adsorption or mass change of the experimental composites was evaluated by immersing them in three storage media that simulate the behavior of different food categories (according to the European Union).[35–37]

10% ethanol = simulant A

3% acetic acid in water = simulant B

20% ethanol in water = simulant C

The adsorbed mass was calculated according to ASTM D570.[38] The immersion media were selected to simulate different categories of food-contact environments. Nine small composite specimens of approximately 5 × 5 × 5 mm were initially weighed (M_0) using an analytical balance with a precision of 0.001 g (Ohaus Explorer, Bucharest, Romania). Three specimens from each batch were immersed in 15 mL of the corresponding simulant solution and stored at ambient temperature (~25 °C) for 6 months (≈182.5 days or 1.58 × 10^7 s). After the immersion period, the specimens were removed from the medium, gently dried with absorbent paper, and weighed again (M_6), each sample was weighed three times. After data collection, descriptive statistical tests (mean, standard deviation) followed by a one-way ANOVA to evaluate statistically significant differences between groups where applied. The percentage of mass change was calculated using the equation:

$$M_{\text{change}} = \frac{M_0 - M_6}{M_0} \times 100$$

Fourier-transform infrared (FTIR) spectroscopy. The chemical bonding of degradation samples was examined by Fourier-transform infrared (FTIR) spectroscopy using an FTIR-610 spectrometer (Jasco Corporation, Tokyo, Japan) equipped with an attenuated total reflectance (ATR) accessory incorporating a horizontal ZnSe crystal (Jasco PRO400S). Spectra were collected over the 4000–500 cm^{-1} range with a resolution of 4 cm^{-1}. Each spectrum represents the average of 100 scans, and all measurements were carried out at room temperature.

Differential scanning calorimetric (DSC). Differential scanning calorimetric (DSC) determination was performed with a DSC 3+ Star system from METTLER TOLEDO (Leicester, UK), under a N2 environment at 10 °C min^{-1} between 25 °C and 200 °C.

Vickers hardness. Vickers hardness measurements were performed to evaluate the mechanical resistance of the polymer composites. Changes in hardness indicate the effect of nanoparticle incorporation and possible degradation during storage.

For hardness measurements of the experimental composites, five values were recorded for each formulation using a Duramin 40 device. According to ASTM E384,[39] Vickers hardness (HV) was determined by applying a load of 100 g for 15 s onto the surface of each specimen, each with a minimum thickness of 3 mm.[40] The mean and standard deviation for each group were calculated using descriptive statistics.

Surface investigations (SEM). Surface investigations were performed using SEM measurements to assess the morphology and the roughness of the polymer composites. These properties are critical for understanding the interaction with food products and the distribution of incorporated nanoparticles.

The morphology of the investigated surfaces, both initially and after immersion in food simulants, was examined using scanning electron microscopy (SEM). The analyses were performed with a Hitachi SU8230 instrument (Hitachi, Tokyo, Japan) operated in high vacuum mode at an acceleration voltage of 30 kV. Images were acquired at increasing magnifications (×500, ×1000, ×2000, ×5000) and a scale of 50 μm was chosen to best lighlight the difference between samples and the effects of degradation.

Antioxidant effect. The antioxidant activity of the polylactic preparations was evaluated using the ABTS cation radical decolorization method.[41] This analysis provides insight into the material's ability to scavenge free radicals, contributing to both the stabilization of the polymer matrix and the protection of food products against oxidative degradation.

In a 96-well plate, 100 μL of each polylactic preparation were mixed with a 214 μM ABTS+• solution in 10 mM HPO_4^{2-} buffer (pH 7.4), to a final volume of 300 μL. Control samples were prepared using only the ABTS˙+ solution, as well as ABTS˙+ mixed with 100 μL of each solvent (A – 10% ethanol; B – 3% acetic acid; C – 20% ethanol). Immediately after mixing, absorbance at 740 nm was measured. All samples were then incubated for four hours in the dark, after which absorbance at 740 nm was measured again.

A calibration curve was prepared using gallic acid (0.2–4 μM), with samples incubated for four hours under the same conditions. The antioxidant activity of lactic acid (3 M) was also tested. The antioxidant activity of the polylactic acid formulations was ex-pressed as gallic acid equivalents. All measurements were performed in duplicate.

Results and discussion

Electron paramagnetic resonance (EPR) analysis

Electron Paramagnetic Resonance (EPR) spectroscopy provided additional insight into the chemical changes and leaching phenomena occurring during immersion. Both the pure solvents and those used for immersion of the undoped PLA samples displayed no discernible EPR signal. In contrast, solvents collected from the doped PLA samples exhibited characteristic signals corresponding to the incorporated dopants.For the Cu^{2+}-doped PLA (R9), an axial copper signal was detected at $g\perp \approx 2.2$ (grey spectra, Fig. 2), confirming the partial migration of copper species into the surrounding medium. The Ag^{+}-doped PLA samples (green spectra, Fig. 2) showed weak signals cor-responding to Mn^{2+} ($g \approx 2.01$).

A stronger manganese signal was observed in the marc-doped PLA samples, particularly those immersed in acetic acid. This can be attributed to the presence of Mn in grape-derived residues and its enhanced extraction under acidic conditions. All solvents collected after PLA immersion exhibited a low-intensity free radical signal, suggesting the formation of

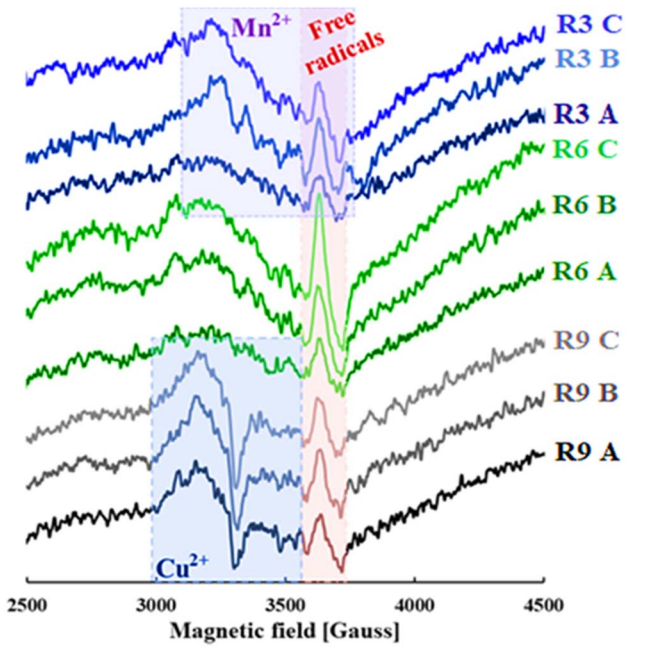

Fig. 2 The cw X-band EPR spectra of Cu^{2+}-doped PLA (R9 in grey), Ag^{+}-doped PLA (R6 in green) and marc-doped PLA (R3 in blue) submerged in ethanol (A and C) and in acetic acid (B). The EPR spectra were measured over 5000 gauss (center field at 2505 gauss) with 40 s sweep time, 3 gauss modulation amplitude and 10 scans. The areas specific for Cu^{2+}, Mn^{2+} and free radicals are high-lighted.

organic radicals during incubation—likely due to mild oxidative degradation of the polymer matrix.

Adsorption at 6 months

C1 (pure PLA1) exhibits very low mass changes (below 0.5%) regardless of the simulant used, suggesting a stable structure that does not dissolve or disintegrate and showing good chemical resistance toward all three food simulants. This confirms the high hydrolytic stability of the base polymer (PLA1) under the tested conditions, in the absence of plasticizers or additives.

The release of metallic elements from the PLA-based composites into simulant A (10% ethanol) and simulant B (3% acetic acid) was quantified after aging tests using ICP-OES measurements.[42] ICP-OES analysis provides the total concentration of metals released into the simulant under the experimental conditions. The measured concentrations therefore correspond to the total metal content present in the solution, which includes dissolved ionic species as well as nanoparticles that may have undergone dissolution during sample preparation and analysis. As reported in the manuscript [42], the amount of migrated material ranged between 0.5–8.5 mg L^{-1} in simulant A and 0.8–16.6 mg kg^{-1} in simulant B, depending on the composite formulation. These results indicate that acidic environments promote a higher release of Cu-containing species, which is consistent with the previously reported behavior of copper-based materials in acidic media.

For C2 (pure PLA 2), the M_{change} values remain low in simulant A (Fig. 3) but exceed 0.7% in simulants B and C, suggesting a reduced resistance of the material to these simulants. This behavior suggests a migration risk, where the solvent penetrates the material and may subsequently release additives into the simulant.[42]

For samples R1–R3, which all contain Proviplast 2624 and grape pomace, negative or near zero M_{change} values were observed in all simulants, indicating a balance between simulant uptake and mass loss processes. Sample R1, with the lowest grape pomace content, exhibits a mass decrease of approximately −2%, suggesting limited swelling combined with partial leaching of low-molecular-weight components, including plasticiser fractions. In contrast, samples R2 and R3, containing higher grape pomace loadings, show mass variations close to zero. This behaviour can be attributed to the increased filler content, which may restrict polymer chain mobility and reduce plasticiser migration, while simultaneously promoting limited simulant absorption through the hydrophilic nature of grape pomace. As a result, simulant uptake and mass loss effects appear to compensate each other in R2 and R3, leading to negligible net mass change rather than enhanced stability alone.[43]

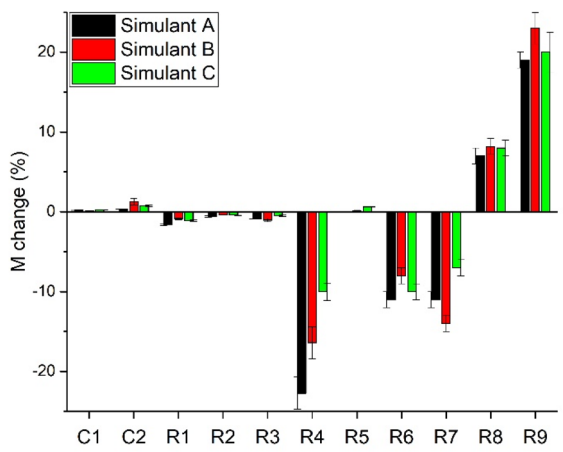

Fig. 3 Amount of mass change after 6 months (≈182.5 days or 1.58 × 10^7 s).

For samples R4–R6, which include Ag-PEG at concentrations ranging from 2% to 8%, more pronounced negative M_{change} values (−10% to −20%) were observed (Fig. 3), with the exception of sample R5, which exhibited negligible mass change. The highest mass losses were recorded for sample R4, particularly in simulant A. These results are consistent with surface degradation phenomena observed by optical microscopy and SEM imaging, including delamination and partial surface dissolution (Fig. 1), which can lead to material loss without involving bulk structural disintegration. For the Cu containing composites (R7–R9), the mass change parameter varied systematically with the copper content. Sample R7 (2% Cu) exhibited a negative M_{change} of −11%, indicating a net mass increase after exposure, which is attributed to increased solvent uptake and swelling of the polymer matrix. In contrast, samples R8 (5% Cu) and R9 (8% Cu) showed positive M_{change} values of +8% and +20%, respectively, reflecting a progressive transition toward net mass loss with increasing filler concentration.

Surface analysis confirmed that samples with higher Cu content developed more pronounced morphological alterations, including localized delamination, microcracking, and partial erosion. These features correlate with the higher positive M_{change} values observed for R8 and R9, suggesting that degradation driven material loss became dominant at elevated Cu levels. In contrast, the lower Cu sample R7 remained structurally more cohesive, allowing solvent retention without significant detachment of fragments, consistent with its negative M_{change} (Fig. 1).[44]

Under typical ambient storage conditions, PLA-based materials generally show relatively slow degradation because hydrolytic chain scission requires the presence of moisture and elevated temperatures. Therefore, if the investigated composites are stored for extended periods (*e.g.*, one to two years) in dry room conditions, only limited degradation is expected. However, gradual physical aging, slow oxidation processes, or the influence of residual moisture may still lead to minor structural or mechanical changes over long storage times. This can temporarily increase the apparent mass. Some PLA composites swell significantly during long-term immersion, leading to pore formation and retention of liquid and low-molecular species.[45]

The higher degradation observed in the PLA2 series can be attributed to its lower molecular weight and lower crystallinity compared to PLA1, which increases chain mobility and the accessibility of ester bonds to hydrolytic attack. Additionally,

the lower melting point of PLA2 facilitates faster polymer chain relaxation during processing and environmental exposure, further promoting hydrolysis.

The observed trend in adsorption (Simulant A > Simulant C > Simulant B) can be attributed to the interactions between the PLA-based composites and the chemical characteristics of the simulants. Simulant A (10% ethanol in water) is moderately polar and can partially swell the PLA matrix, leading to higher adsorption.

In contrast, Simulant C (20% ethanol in water), with a higher ethanol content, exhibits reduced hydrogen bonding interactions with PLA ester groups, resulting in slightly lower adsorption. Simulant B (3% acetic acid in water) is acidic but poorly polar, interacting minimally with the polymer matrix and thus showing the lowest adsorption. Moreover, the presence of hydrophilic additives such as grape pomace or Ag-PEG/Cu-Peg enhances the uptake of water/ethanol, while their dispersion and morphology influence the diffusion pathways within the composite.

A one-way ANOVA confirmed significant differences in mass variation across the samples ($p < 0.05$).

Vickers hardness

The Vickers hardness results for all samples are shown in Fig. 4.

Fig. 5 provides a scientific interpretation of the correlation between M_{change} and Vickers hardness, evaluated as a function of the samples' exposure to the three food simulants (A/B/C). From a mechanistic perspective, the sign and magnitude of M_{change} indicate the dominant interaction processes between the polymer and the simulant.

The slopes of the regression lines (R^2) for each simulant quantify the sensitivity of hardness to mass variation in that medium. A steeper slope (accompanied by a higher R^2) suggests that the operative mechanisms in that simulant exert tighter control over the evolution of the mechanical properties: the more consistent the mass loss, the stronger the response. A modest R^2 indicates multivariable behavior, in which HV is simultaneously influenced by additional factors such as compositional heterogeneity, initial microstructure, and the presence/agglomeration of the filler.

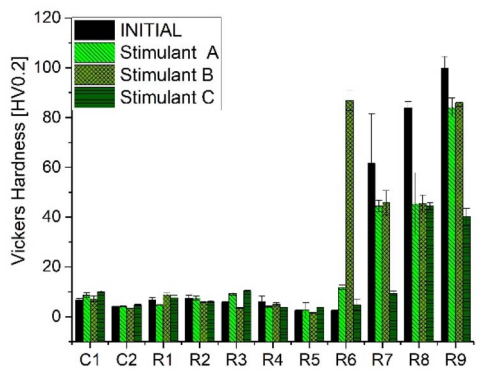

Fig. 4 Vickers hardness of the samples before and after immersion in Stimulant A, B, and C.

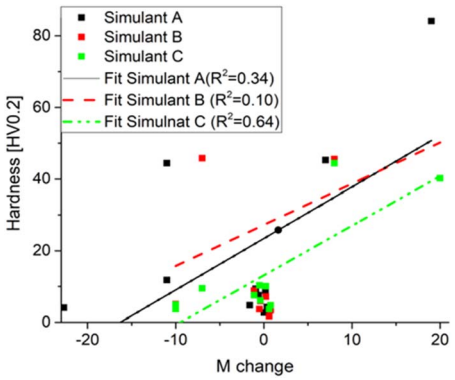

Fig. 5 Relationship between mass change and Vickers hardness across food simulants.

If the data sets for one simulant tend to align along the same regression line with a higher R^2, we infer that the phenomenology is more coherent (*e.g.*, the predominance of the same type of transport/dissolution/erosion mechanism across all samples). If the points are more scattered and the regression is weak, this means that local micro mechanisms (*e.g.*, filler distribution, surface roughness, residual stresses, degree of crystallinity) modulate the mechanical response more strongly than mass variation itself. Overall, the figure integrates the significance of M_{change} (an integrative indicator of polymer–simulant interaction) with HV (a proxy for local scale mechanical integrity), providing a mechanistic map: as the system transitions from swelling to mass loss, hardness tends to decrease, and the "strength" of the correlation depends on the nature of the simulant and the composite's microstructure.

PLA 1 was more crystalline and rigid, exhibiting higher initial hardness than PLA 2. After six months of immersion, the hardness of PLA 1 increased across all media. This can be attributed to the selling and adsorption processes of the polymer, which result in stiffer specimens.

For samples R1, R2, and R3, a similar trend was observed, with slightly lower hardness values than the control samples due to the plasticizer's softening effect. However, as the amount of grape pomace powder increased, the hardness of the specimens also slightly increased surpassing that of pure PLA 1 for R3, which contained 1.5% grape pomace. Thus, grape pomace acts as a bio-solid filler which, at low concentrations (0.5–1.5%), can slightly enhance the modulus and hardness when it adheres well to the polymer matrix, thereby counteracting the plasticizer's influence.

For samples R4–R9, the initial hardness increased with higher Cu particle content (for R7-R9), but decreased with increasing Ag concentration (for R4-R7). Cu nanoparticles acted as crystallization nuclei, reinforcing the material's stiffness, whereas Ag particles if poorly dispersed or weakly bonded created defect zones that reduced hardness and strength.

After six months of immersion, these samples showed a decrease in hardness due to diffusion of small molecules, where plasticizers or additives were extracted by the simulants. This process led to delamination and microcrack formation within the composite structure.

A strong correlation was observed between M_{change} and Vickers hardness, both reflecting physicochemical changes in the polymer matrix. In samples R1–R3, negative M_{change} values coincided with increased hardness indicating limited degradation, simulant adsorption, and densification of the structure. In contrast, samples R4–R6 and R7–R9 transitioned from negative to positive M_{change} values (exceeding 1%), showing that nanoparticle content significantly influenced behavior over six months of immersion. Hardness decreased moderately compared to the initial values, corresponding to structural degradation through phase loss, partial dissolution (R6, R9), and delamination (R5, R8). The overall degree of degradation in these materials was substantial.

Surface investigations (SEM)

SEM micrographs of the sample surfaces after six months of immersion in the three food simulants (A–C) are shown in Fig. 6–9. In the images, black circles mark particulate features visible at the surface, while arrows indicate cracks and surface defects of different sizes and morphologies.[46] The observations below are based on surface morphology and do not provide direct information on the internal dispersion of fillers or nanoparticles.

Simulant A (10% ethanol in water). After immersion in the mildly hydroalcoholic medium, neat PLA shows slight surface roughening and fine microcracks, indicative of surface localized hydrolytic processes without evidence of bulk erosion—

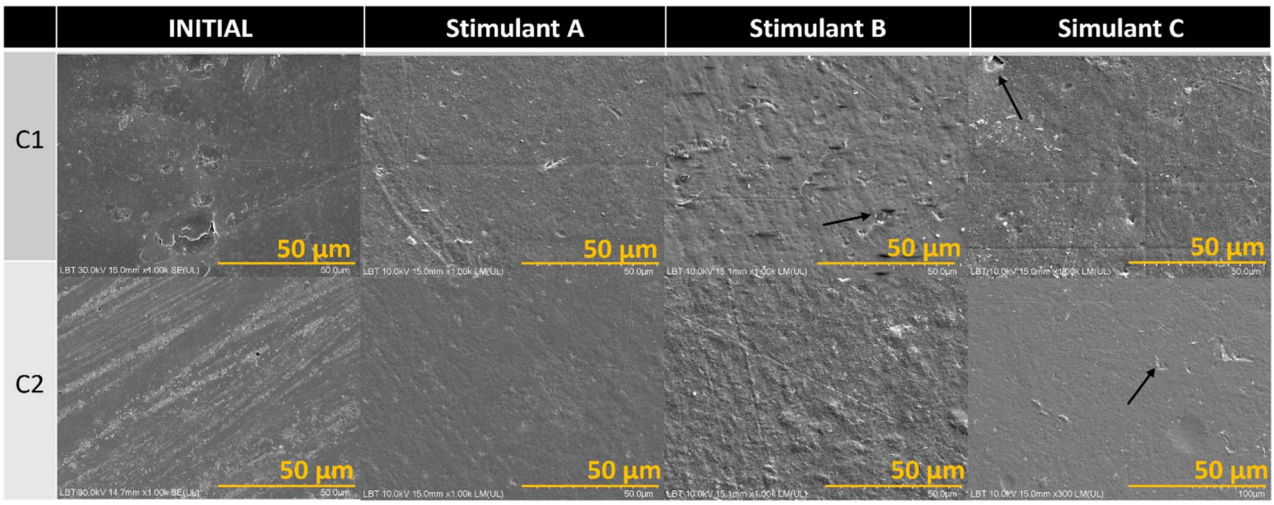

Fig. 6 SEM images of the control samples before and after 6 months of immersion in food simulants.

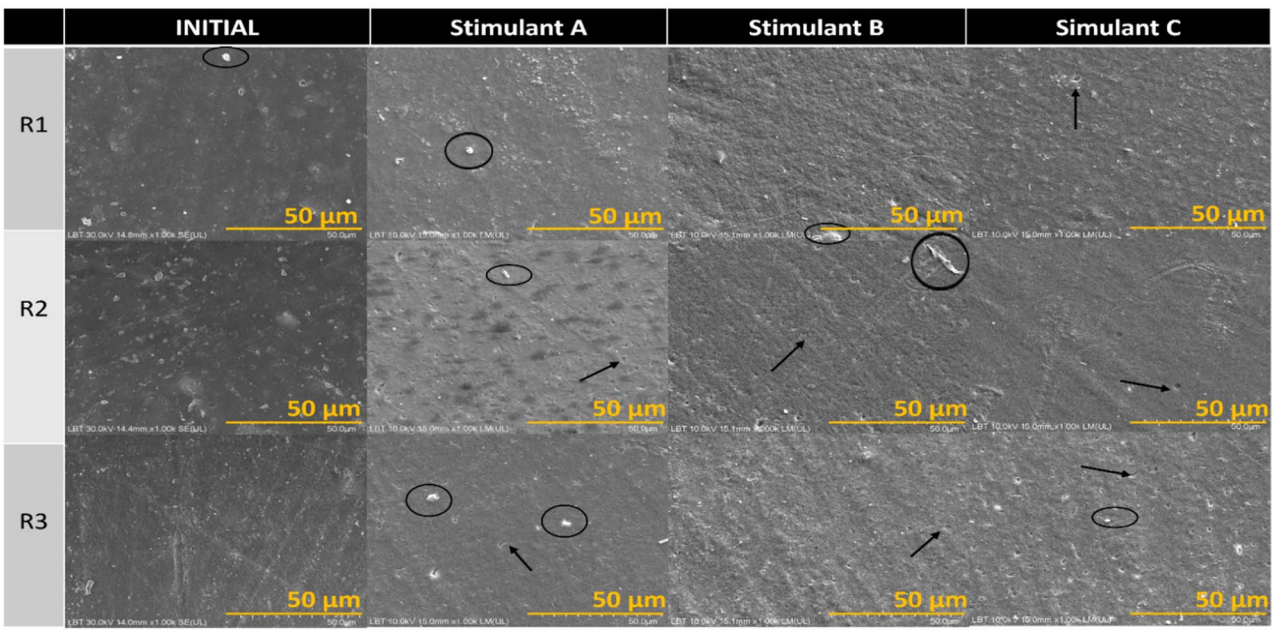

Fig. 7 SEM images of R1-R3 before and after 6 months of immersion in food simulants.

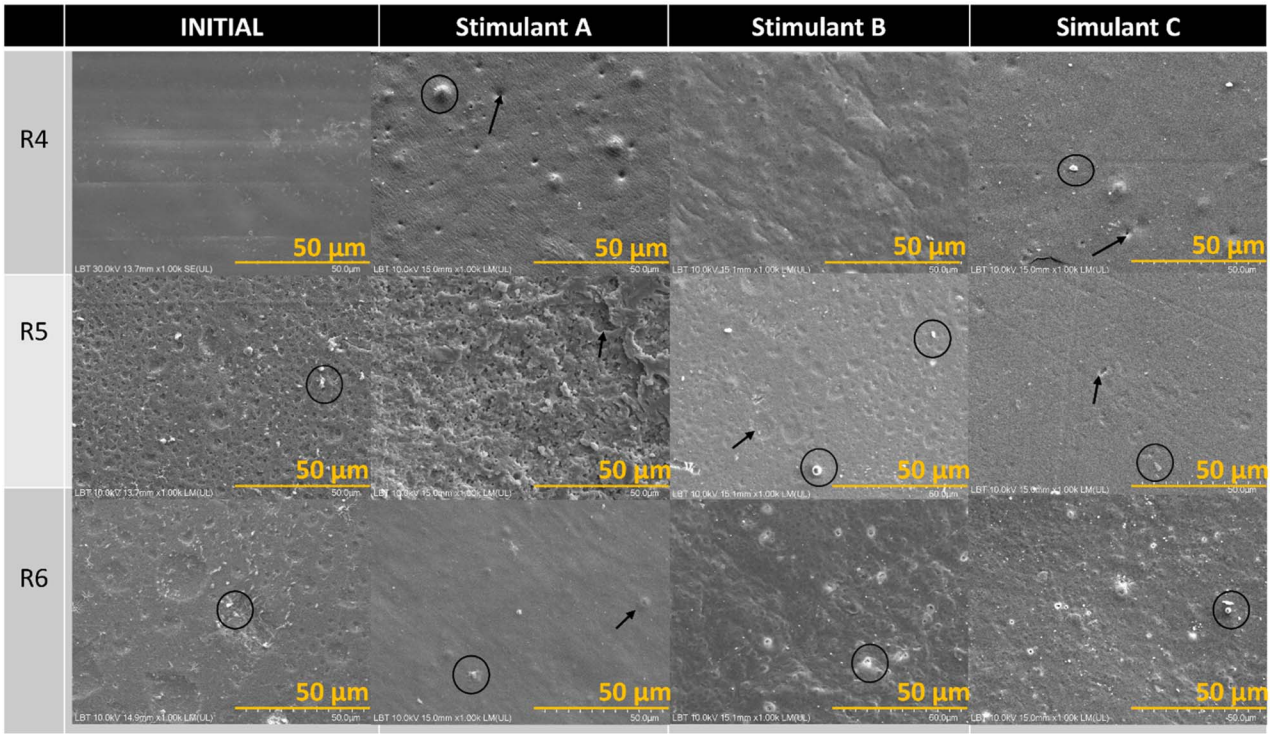

Fig. 8 SEM images of R4-R6 samples before and after 6 months of immersion in food simulants.

consistent with the near zero mass change measured under these conditions. For the PLA–grape pomace composites, ethanol appears to promote mild swelling of the organic inclusions and partial diffusion of low molecular weight components. SEM reveals shallow fissures and small interfacial voids, attributable to localized interfacial stresses between the PLA matrix and dispersed pomace particles; no filler detachment is observed, aligning with their minimal mass change. In the PLA–Ag PEG and PLA–Cu PEG nanocomposites, the surfaces remain largely compact, with occasional fine voids and isolated defects consistent with localized matrix relaxation or superficial restructuring. While particulate features are visible, SEM alone cannot confirm nanoparticle distribution or migration. Overall, simu-lant A induces minor, surface limited changes consistent with low M_{change}.

Simulant B (3% acetic acid in water). Immersion in the acidic simulant leads to more pronounced surface deterioration across all materials. Neat PLA displays erosion patterns and deeper surface cracks, consistent with acid catalyzed hydrolysis and surface chain scission, and in line with higher mass loss. In the PLA–grape pomace composites, acetic acid intensifies attack on the organic phase, resulting in enlarged interfacial gaps and regions with flaked/eroded texture, indicating preferential degradation at the polymer–filler interface. The nanocomposites show the most severe surface damage in this environment. PLA–Cu PEG specimens exhibit copper species under acidic conditions (enhanced hydrolysis/redox mediated pathways). PLA–Ag PEG samples display similar but less pronounced deterioration. Among the three simulants, acetic acid produces the strongest coupling between erosive morphology and mass loss.extensive surface fragmentation and irregular cavities, features consistent with accelerated surface degradation in the presence of Simulant C (20% ethanol in water).

All materials exhibit marked increases in roughness and porosity, reflecting the stronger solvent action of ethanol and enhanced mobility of low molecular weight species. Neat PLA shows widened cracks and a sponge-like surface, suggesting softening/reorganization within amorphous regions. In the PLA–grape pomace composites, ethanol interacts with organic constituents, leading to swelling, extraction of soluble fractions, and microcavity formation. For the nanocomposites, the higher ethanol content promotes matrix relaxation and surface erosion, yielding heterogeneous surfaces with eroded zones and small cavities where particulate features appear detached. Without complementary elemental analyses, these features cannot be directly attributed to nanoparticle redistribution or leaching. Notably, samples such as R5 (and similarly R8) show pronounced surface roughening alongside minimal mass change, indicating surface confined swelling/softening and localized reorganization that strongly impact SEM visible morphology but contribute little to the overall mass balance.

Consistency with mass change results. The SEM observations are consistent with the measured mass changes: low M_{change} corresponds to swelling dominated, surface limited alterations (fine fissures, roughening, shallow voids) that do not imply net material removal, whereas conditions with measurable mass loss are accompanied by erosive morphologies (deeper cracks, fragmented regions, enlarged interfacial gaps) indicative of surface recession. Ethanol rich exposure (simulant C) can thus reshape the surface without appreciable mass change, while acetic acid (simulant B) produces the most aggressive, mass loss consistent surface damage.

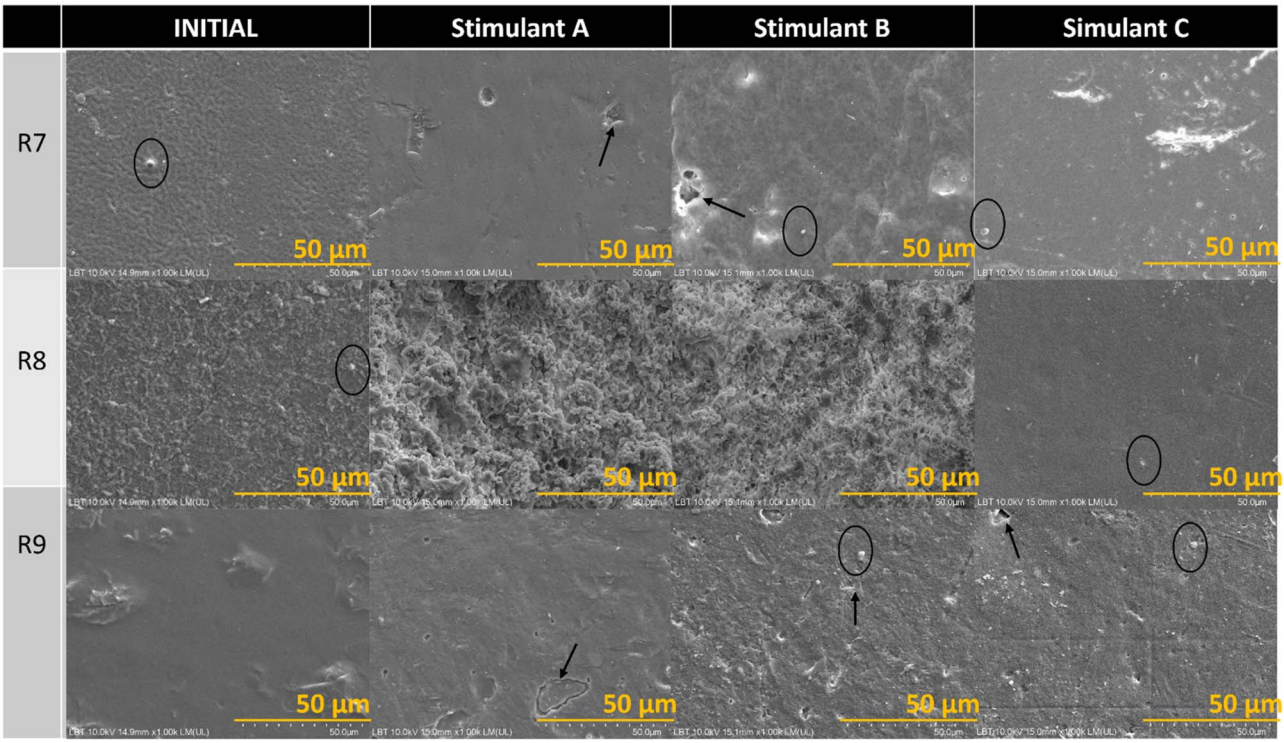

Fig. 9 SEM images of R7-R9 samples before and after 6 months of immersion in food simulants.

FTIR spectroscopy analysis

FTIR analysis (Fig. 10) was performed after six months of immersion in food simulants (10% ethanol, 3% acetic acid, and 20% ethanol) to assess potential chemical changes occurring during prolonged exposure.

FTIR spectra (Fig. 10) of the PLA-based composites show the characteristic absorption bands of PLA, including the C=O

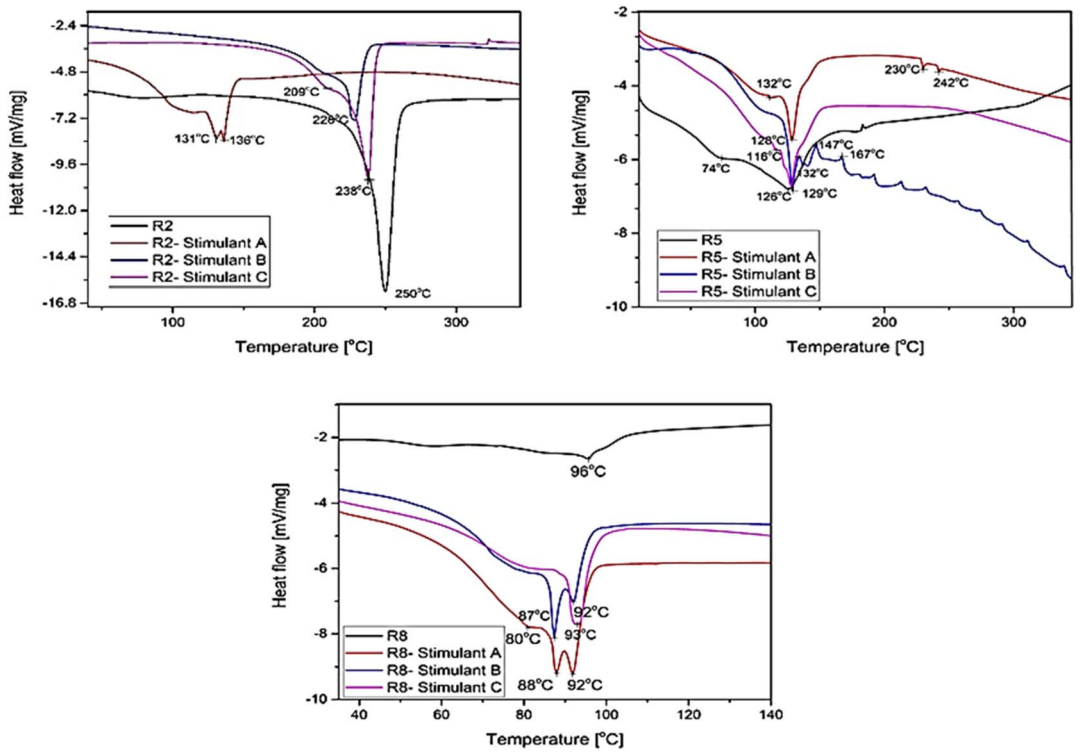

Fig. 10 FTIR analysis (initial and after six months of immersion in food simulants).

stretching vibration around 1750 cm^{-1}, C–O–C stretching bands between 1180–1080 cm^{-1}, and CH_3 stretching vibrations near 2990–2945 cm^{-1}. These peaks confirm the presence of the PLA matrix in all formulations. After incorporation of grape pomace powder or Ag-PEG/Cu-PEG nanofillers, slight changes in peak intensity and small shifts in some bands are observed, indicating interactions between the PLA matrix, plasticizer (Proviplast 2624), and the fillers. Additional bands associated with hydroxyl groups (–OH) from grape pomace may appear around 3200–3500 cm^{-1}, suggesting hydrogen bonding interactions with PLA. Following six months of immersion in food simulants (10% ethanol, 3% acetic acid, and 20% ethanol), minor variations in band intensity were detected.

These changes may be attributed to plasticizer migration, solvent absorption, or slight hydrolytic degradation of the PLA matrix. However, the main characteristic PLA bands remain present, indicating that the overall chemical structure of the composites is preserved after exposure. Changes observed in the carbonyl stretching region and in other characteristic PLA bands indicate alterations in the chemical environment of ester groups, which are consistent with hydrolytic cleavage of the polymer backbone

DSC analysis

The samples (Fig. 11) were immersed for six months in food simulants (10% ethanol, 3% acetic acid, and 20% ethanol) and then analyzed by DSC to evaluate changes in thermal behavior (Fig. 10). The DSC thermograms reveal that the addition stimulants significantly alter the thermal behavior of R2, R5, and R8 formulations. For R2, the pure sample shows a major endothermic peak at ~250 °C, corresponding to its primary thermal degradation. The introduction of stimulants shifts this peak to lower temperatures, indicating reduced thermal stability. Stimulant A induces multiple early transitions (≈131–209 °C), suggesting strong interactions and early decomposition processes. Stimulants B and C show peaks closer to the original degradation temperature (≈228–238 °C), indicating comparatively weaker but still noticeable effects.

In R5, thermal events occur at lower temperatures (≈74–116 °C), reflecting inherently lower stability than R2. The addition of stimulants increases the number of transitions, particularly for stimulant B, which exhibits a multi-step decomposition pattern. This suggests more complex interactions and progressive structural or chemical changes within the matrix.

For R8, all transitions occur below 100 °C, indicating the lowest thermal stability among the samples. Stimulants further shift and intensify endothermic peaks (≈80–93 °C), confirming enhanced interactions and earlier thermal events. DSC analysis revealed changes in the thermal behaviour of PLA after prolonged exposure. Variations in the glass transition temperature (Tg), melting temperature (Tm), and crystallinity suggest structural rearrangements associated with polymer chain scission and possible recrystallization during degradation. Such behaviour is consistent with hydrolysis-driven degradation mechanisms commonly reported for PLA, where preferential cleavage of amorphous regions leads to increased chain mobility and potential crystallinity evolution.

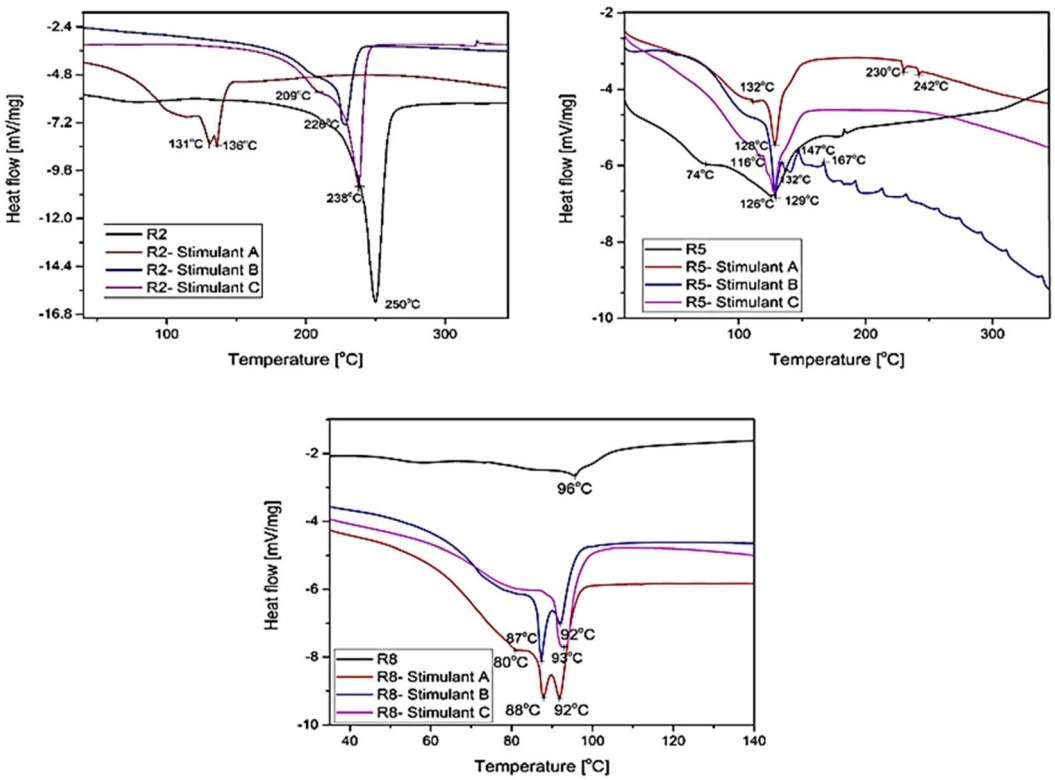

Fig. 11 DSC analysis (initial and after six months of immersion in food simulants).

Across all systems, stimulants, shift thermal transitions to lower temperatures, increase the number of endothermic events and indicate multi-step decomposition or phase transitions. The overall thermal stability follows: R2 > R5 > R8.

Antioxidant activity

The antioxidant capacity was evaluated exclusively in the solvents collected after the 6 month immersion period, using the $ABTS^{\bullet+}$ decolorization assay. Therefore, the results do not reflect the intrinsic antioxidant properties of the PLA-based materials themselves, but rather the antioxidant activity of compounds released into the surrounding liquids during storage. Baseline antioxidant activity of the fresh simulants prior to immersion was negligible and was used as a reference control.

Most post-immersion solvent samples, particularly those corresponding to acetic acid (simulant B) and to Cu^{2+}- and Ag^{+}-doped PLA materials, exhibited no detectable antioxidant activity.

This observation suggests either the absence of antioxidant compounds in the leachates or a possible loss of activity during the prolonged incubation period.

In contrast, solvents obtained from undoped PLA samples immersed in ethanol-based simulants (A and C) displayed measurable antioxidant activity, reaching values of up to 5 GAE (Fig. 12). Given that lactic acid itself exhibits negligible antioxidant capacity (0.02 GAE), this activity is likely attributable to the release of minor organic residues or processing-related additives from the PLA matrix rather than to PLA degradation products.

The highest antioxidant activity was observed for solvents from marc-doped PLA samples immersed in ethanol, with values ranging from 6.7 to 11 GAE. This pronounced response is consistent with the release of polyphenolic compounds from grape marc during the incubation period.[47] The use of gallic acid as a calibration standard—chosen due to its abundance in grape-derived extracts (Fig. S2) —further supports this interpretation.

The differences in antioxidant activity among the samples arise from the combined effects of material composition, solvent environment, and the chemical stability of released species. The higher antioxidant response of sample C2 compared to C1 is attributed to the increased ethanol content in simulant C, which enhances PLA swelling and pro-motes the extraction of low-molecular-weight organic residues with limited radical scavenging ability.

Among the marc-doped materials, measurable antioxidant activity was observed only for sample R3. This behaviour is consistent with a higher effective release of pomace derived polyphenolic compounds within the polymer matrix, resulting in activity below the detection limit of the $ABTS^{\bullet+}$ assay.

Although Fig. 12 indicates the presence of pomace-associated metal cations in all simulants for sample R3, their detection does not necessarily imply preserved antioxidant activity. In simulant B (3% acetic acid), acidic conditions can promote oxidation, hydrolysis, or metal complexation of polyphenols, thereby suppressing their radical-scavenging efficiency. In addition, released metal ions may exhibit prooxidant behaviour under acidic conditions, further counteracting antioxidant effects. Consequently, despite the presence of pomace-derived components in simulant B, no measurable antioxidant activity is detected.

Overall, antioxidant activity depends not only on the release of pomace derived species but also on their chemical integrity and reactivity within each simulant. Ethanol based environments preserve polyphenolic functionality and allow detectable antioxidant responses, whereas acidic conditions inhibit or neutralize this activity.

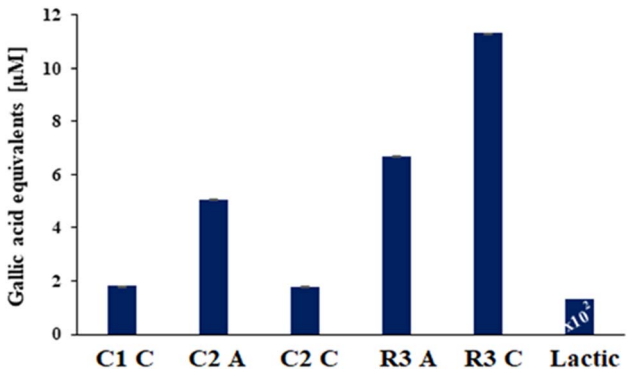

Fig. 12 The gallic acid equivalents of each PLA-based formulation determined with the ABTS cation radical quenching after four hours of incubation. Only PLAs that display antioxidant activity are shown.

Correlation between morphological and chemical changes

The combined SEM and EPR analyses indicate that the degradation behaviour of the investigated PLA systems is strongly influenced by the nature of the immersion medium. The acidic environment (simulant B) promotes polymer chain scission and redox-related degradation processes, resulting in more pronounced surface damage observed by SEM and increased paramagnetic signals detected by EPR. In contrast, ethanol-containing simulants (A and C) facilitate the diffusion and extraction of low-molecular-weight organic compounds and potential nanoparticulate species from the polymer matrix.

The antioxidant activity detected in the ethanolic simulants supports the release of bioactive polyphenolic compounds, particularly from the marc-doped composites. This indicates that the simulant composition not only affects the degradation kinetics of PLA but also influences the chemical profile and potential bioactivity of the released species.

Overall, the correlation between mass variation, hardness evolution, SEM-observed surface morphology, EPR signals, and complementary FTIR and DSC analyses suggests that degradation is primarily governed by hydrolysis-induced chain scission of the PLA backbone. Secondary oxidative processes may occur during prolonged exposure, contributing to radical formation and additional chemical modifications of the polymer matrix.

Although PLA is widely considered a promising biodegradable polymer for food packaging, it still exhibits several limitations, including limited ductility, moderate thermal stability, and sensitivity to hydrolytic degradation. The results obtained

in this study indicate that the incorporation of grape pomace and metallic nanofillers can partially improve the structural stability and mechanical response of PLA composites under simulated food-contact conditions. In particular, the grape pomace filler contributed to increased hardness and dimensional stability, while Ag-PEG and Cu-PEG nanofillers improved nanoparticle dispersion and influenced the degradation behaviour of the polymer matrix.

Conclusions

PLA-based nanocomposites containing grape marc or metallic nanoparticles (Ag and Cu) were investigated after six months of exposure to selected food simulants to evaluate changes in surface morphology, hardness, chemical structure, and radical formation. The results indicate that both the composite formulation and the nature of the simulant strongly influence the extent and characteristics of material degradation. Grape marc–reinforced composites exhibited increased Vickers hardness after immersion, particularly in ethanolic simulants, which can be attributed to the rigid filler effect and moisture-induced microstructural changes. These samples also showed measurable antioxidant activity in ethanol, consistent with the release of phenolic compounds from the plant-based filler.

In contrast, Ag-PEG and Cu-PEG nanocomposites displayed limited antioxidant activity. EPR analysis revealed radical species formation associated with polymer degradation and metal–polymer redox interactions rather than leaching of antioxidant compounds. FTIR spectroscopy provided evidence of chemical modifications in the PLA matrix, including hydrolysis of ester groups, while DSC measurements indicated changes in glass transition, melting behavior, and crystallinity, reflecting structural rearrangements during exposure. Among the tested simulants, acetic acid induced the most pronounced surface degradation and polymer fragmentation, as confirmed by SEM, EPR, FTIR, and DSC analyses.

Overall, the findings highlight that both immersion media and additive type significantly affect the degradation behavior, chemical structure, and surface-related properties of PLA-based composites. These results provide comparative insight into additive–simulant interactions, while further time-dependent, mechanical, and molecular analyses would be required to establish quantitative correlations and define application-specific performance criteria.

Author contributions

Conceptualization, O. N. and A. M.; methodology, S. C. and V. P.; software, I. S.; validation, R. S. D. and O. N; formal analysis, C. Z. T.; investigation, C. S., C. Z. T. and A. T.; resources, A. M.; data curation, C. S.; writing—original draft preparation, S. C.; writing—review and editing, O. N.; visualization, V. P. All authors have read and agreed to the published version of the manuscript.

Conflicts of interest

There are no conflicts to declare.

Data availability

Processed data supporting the findings of this study (mean values and standard deviations) are provided in the manuscript and the supplementary information (SI). The full raw datasets, including all recorded SEM images and all individual measurement results used for statistical analysis, are available from the corresponding author upon reasonable request for verification purposes. Supplementary information is available. See DOI: https://doi.org/10.1039/d6ra01374k.

Notes and references

1 T. A. Swetha, A. Bora, K. Mohanrasu, P. Balaji, R. Raja, K. Ponnuchamy, G. Muthusamy and A. Arun, A comprehensive review on polylactic acid (PLA)–Synthesis, processing and application in food packaging, *Int. J. Biol. Macromol.*, 2023, **234**, 123715, DOI: 10.1016/j.ijbiomac.2023.123715.

2 N. S. A. Malek, M. Faizuwan, Z. Khusaimi, N. N. Bonnia, M. Rusop and N. A. Asli, Preparation and characterization of biodegradable polylactic acid (PLA) film for food packaging application: A Review, *J. Phys.:Conf. Ser.*, 2021, **1892**, 012037, DOI: 10.1088/1742-6596/1892/1/012037.

3 J. O'Loughlin, D. Doherty, B. Herward, C. McGleenan, M. Mahmud, P. Bhagabati, A. N. Boland, B. Freeland, K. D. Rochfort, S. M. Kelleher, S. Fahy and J. Gaughran, The potential of bio-based polylactic acid (PLA) as an alternative in reusable food containers: a review, *Sustainability*, 2023, **15**(21), 15312, DOI: 10.3390/su152115312.

4 A. Panou and I. K. Karabagias, Biodegradable packaging materials for foods preservation: sources, advantages, limitations, and future perspectives, *Coatings*, 2023, **13**(7), 1176, DOI: 10.3390/coatings13071176.

5 L. K. Ncube, A. U. Ude, E. N. Ogunmuyiwa, R. Zulkifli and I. N. Beas, Environmental impact of food packaging materials: A review of contemporary development from conventional plastics to polylactic acid-based materials, *Materials*, 2020, **13**(21), 4994, DOI: 10.3390/ma13214994.

6 H. YousefniaPasha, S. S. Mohtasebi, R. Tabatabaeekoloor, M. Taherimehr, A. Javadi and M. Soltani Firouz, Preparation and characterization of the plasticized polylactic acid films produced by the solvent-casting method for food packaging applications, *J. Food Process. Preserv.*, 2021, **45**(12), e16089, DOI: 10.1111/jfpp.16089.

7 F. Akoueson, I. Paul-Pont, K. Tallec, A. Huvet, P. Doyen, A. Dehaut and G. Duflos, Additives in polypropylene and polylactic acid food packaging: Chemical analysis and bioassays provide complementary tools for risk assessment, *Sci. Total Environ.*, 2023, **857**, 159318, DOI: 10.1016/j.scitotenv.2022.159318.

8 C. Villegas, M. P. Arrieta, A. Rojas, A. Torres, S. Faba, M. J. Toledo, M. A. Gutierrez, E. Zavalla, J. Romero, M. J. Galotto and X. Valenzuela, PLA/Organoclay Bionanocomposites Impregnated with Thymol and Cinnamaldehyde by Supercritical Impregnation for Active

and Sustainable Food Packaging, *Composites, Part B*, 2019, **176**, 107336, DOI: 10.1016/j.compositesb.2019.107336.

9 M. D. Chomachayi, A. Jalali-arani, F. R. Beltrán, M. U. de la Orden and J. M. Urreaga, Biodegradable Nanocomposites Developed from PLA/PCLBlends and Silk Fibroin Nanoparticles: Study on the Microstructure, Thermal Behavior, Crystallinity and Performance, *J. Polym. Environ.*, 2020, **28**, 1252–1264, DOI: 10.1007/s10924-020-01684-0.

10 K. Martinez Villadiego, M. J. Arias Tapia, J. Useche and D. Escobar Macías, Thermoplastic starch (TPS)/polylactic acid (PLA) blending methodologies: A review, *J. Polym. Environ.*, 2022, **30**(1), 75–91, DOI: 10.1007/s10924-021-02207-1.

11 A. Srisa and N. Harnkarnsujarit, Polyethylene glycol enhanced antibacterial activity of EDTA and ethyl maltol blended PLA against Staphylococcus aureus for biodegradable active packaging, *Food Biosci.*, 2024, **62**, 105237, DOI: 10.1016/j.fbio.2024.105237.

12 M. Thakur, I. Majid, S. Hussain and V. Nanda, Poly (ε-caprolactone): A potential polymer for biodegradable food packaging applications, *Packag. Technol. Sci.*, 2021, **34**(8), 449–461, DOI: 10.1002/pts.2572.

13 J. C. Andrade Chapal, Biodegradable materials based on poly (vinyl alcohol)(PVA) and poly (lactic acid)(PLA) with antioxidant and antimicrobial activity for food packaging applications, Doctoral dissertation, Universitat Politècnica de València, 2021.

14 M. K. Patel, M. Zaccone, L. De Brauwer, R. Nair, M. Monti, V. Martinez-Nogues, A. Frache and K. Oksman, Improvement of poly (lactic acid)-poly (hydroxy butyrate) blend properties for use in food packaging: processing, structure relationships, *Polymers*, 2022, **14**(23), 5104, DOI: 10.3390/polym14235104.

15 A. Nazrin, S. M. Sapuan, M. Y. M. Zuhri, R. A. Ilyas, R. Syafiq and S. F. K. Sherwani, Nanocellulose reinforced thermoplastic starch (TPS), polylactic acid (PLA), and polybutylene succinate (PBS) for food packaging applications, *Front. Chem.*, 2020, **8**, 213, DOI: 10.3389/fchem.2020.00213.

16 I. Chrysafi, N. M. Ainali and D. N. Bikiaris, Thermal degradation mechanism and decomposition kinetic studies of poly (Lactic acid) and its copolymers with poly (hexylene succinate), *Polymers*, 2021, **13**(9), 1365, DOI: 10.3390/polym13091365.

17 M. Ferdinánd, R. Várdai, J. Móczó and B. Pukánszky, A novel approach to the impact modification of PLA, *Eng. Fract. Mech.*, 2023, **277**, 108950, DOI: 10.1016/j.engfracmech.2022.108950.

18 S. B. Munteanu and C. Vasile, Vegetable additives in food packaging polymeric materials, *Polymers*, 2019, **12**(1), 28, DOI: 10.3390/polym12010028.

19 B. Ozalp Ozen and A. Soyer, Effect of plant extracts on lipid and protein oxidation of mackerel (Scomber scombrus) mince during frozen storage, *J. Food Sci. Technol.*, 2018, **55**(1), 120–127, DOI: 10.1007/s13197-017-2847-6.

20 K. Saral Sarojini, M. P. Indumathi and G. R. Rajarajeswari, Mahua oil-based polyurethane/chitosan/nano ZnO composite films for biodegradable food packaging applications, *Int. J. Biol. Macromol.*, 2019, **124**, 163–174, DOI: 10.1016/j.ijbiomac.2018.11.195.

21 E. Sogut and A. C. Seydim, The effects of Chitosan and grape seed extract-based edible films on the quality of vacuum packaged chicken breast fillets, *Food Packag. Shelf Life*, 2018, **18**, 13–20, DOI: 10.1016/j.fpsl.2018.07.006.

22 X. Zhou, X. Zhou, L. Zhou, M. Jia and Y. Xiong, Nanofillers in novel food packaging systems and their toxicity issues, *Foods*, 2024, **13**(13), 2014, DOI: 10.3390/foods13132014.

23 A. Kawale, S. Shukla, V. Thiruvengadam and A. Bansod, Development of silver nanoparticles infiltrated PLA films for food packaging, *Plast., Rubber Compos.*, 2025, **54**(3–4), 82–95, DOI: 10.1177/14658011241304381.

24 N. P. Rybalchenko, V. L. Demchenko, T. T. Hnatiuk, O. M. Vasyliuk, M. V. Iurzhenko, T. V. Rybalchenko, I. O. Sytnyk, D. V. Shtepa and A. I. Marynin, Antimicrobial Effect of Biopolymer Packaging Materials with Silver Nanoparticles for Food Storage, *Microbiol. J.*, 2024, **86**(6), 30–41, DOI: 10.15407/microbiolj86.06.030.

25 A. Istiqola and A. Syafiuddin, A review of silver nanoparticles in food packaging technologies: Regulation, methods, properties, migration, and future challenges, *J. Chin. Chem. Soc.*, 2020, **67**(11), 1942–1956, DOI: 10.1002/jccs.202000179.

26 B. Kuswandi and M. Moradi, in *Improvement of Food Packaging Based on Functional Nanomaterial*, ed. S. Siddiquee, G. Melvin, M. Rahman, Springer, Cham, Switzerland, edition 1, 2019, Nanotechnology: Applications in Energy, Drug and Food, pp. 309–344, DOI: 10.1007/978-3-319-99602-8_16.

27 M. A. Ávila-López, E. Luévano-Hipólito and L. M. Torres-Martínez, CO2 adsorption and its visible-light-driven reduction using CuO synthesized by an eco-friendly sonochemical method, *J. Photochem. Photobiol., A*, 2019, **382**, 111933, DOI: 10.1016/J.JPHOTOCHEM.2019.111933.

28 S. P. Kamble and V. D. Mote, Structural, optical and magnetic properties of Co doped CuO nano-particles by sol-gel auto combustion technique, *Solid State Sci.*, 2019, **95**, 105936, DOI: 10.1016/J.SOLIDSTATESCIENCES.2019.105936.

29 E. M. M. Ibrahim, L. H. Abdel-Rahman, A. M. Abu-Dief, A. Elshafaie, S. K. Hamdan and A. M. Ahmed, The synthesis of CuO and NiO nanoparticles by facile thermal decomposition of metal-Schiff base complexes and an examination of their electric, thermoelectric and magnetic properties, *Mater. Res. Bull.*, 2018, **107**, 492–497, DOI: 10.1016/J.MATERRESBULL.2018.08.020.

30 C. V. Garcia, G. H. Shin and J. T. Kim, Metal oxide-based nanocomposites in food packaging: Applications, migration, and regulations, *Trends Food Sci. Technol.*, 2018, **82**, 21–31, DOI: 10.1016/J.TIFS.2018.09.021.

31 https://biobasedinkopen.nl/app/uploads/2022/04/Safety-Data-Sheet-Luminy-PLA-Neat-resin-22-04-2021.pdf.

32 https://www.specialchem.com/polymer-additives/product/proviron-proviplast-2624.

33 V. Popescu, D. Prodan, S. Cuc, C. Saroși, G. Furtos, A. Moldovan, R. Carpa and D. Bomboș, Antimicrobial poly

(lactic acid)/copper nanocomposites for food packaging materials, *Materials*, 2023, **16**(4), 1415, DOI: 10.3390/ma16041415.

34 K. Shameli, M. Bin Ahmad, S. D. Jazayeri, S. Sedaghat, P. Shabanzadeh, H. Jahangirian, M. Mahdavi and Y. Abdollahi, Synthesis and Characterization of Polyethylene Glycol Mediated Silver Nanoparticles by the Green Method, *Int. J. Mol. Sci.*, 2012, **13**, 6639–6650, DOI: 10.3390/ijms13066639.

35 European Comission, *Commission Regulation (EU) No 10/2011 of 14 January 2011 on Plastic Materials and Articles Intended to Come into Contact with Food; European Comission: Brussels, Belgium*, 2011.

36 S. Yenidoğan, C. Aydemir and C. E. Doğan, Packaging–Food Interaction and Chemical Migration, *Cellul. Chem. Technol.*, 2023, **57**, 1029–1040.

37 S. A. Eti, M. S. Islam, J. H. Shourove, B. Saha, S. K. Ray, S. Sultana, M. A. A. Shaikh and M. M. Rahman, Assessment of heavy metals migrated from food contact plastic packaging: Bangladesh perspective, *Heliyon*, 2023, **9**(9), 19667, DOI: 10.1016/j.heliyon.2023.e19667.

38 *ASTM D790-07; Standard Test Methods for Flexural Properties of Unbreinforced and Reinforced Plastics and Electrical Insulating Materials*, ASTM International, West Conshohocken, PA, USA, 2018.

39 *ASTM E384-22 Standard Test Method for Microindentation Hardness of Materials*, 2022.

40 S. A. Ali, Mechanical and thermal properties of promising polymer composites for food packaging applications, *IOP Conf. Ser.:Mater. Sci. Eng.*, 2016, **137**(1), 012035, DOI: 10.1088/1757-899X/137/1/012035.

41 R. Re, A. Pellegrini, A. Proteggente, A. Pannala, M. Yang and C. Rice-Evans, Antioxidant activity applying an improved ABTS radical cation decolorization assay, *Free Radical Biol. Med.*, 1999, **26**(9–10), 1231–1237, DOI: 10.1016/s0891-5849(98)00315-3.

42 A. Moldovan, S. Cuc, I. Petean, I. S. L. B. Tudoran, R. Carpa, I. Perhaiţa, O. Nemeş, D. Popa, *et al.*, Biodegradability of selected poly(lactic acid) composites for sustainable food packaging applications, *Mater. Degrad.*, 2026, **10**, 12, DOI: 10.1038/s41529-025-00724-1.

43 H. Velichkova, I. Petrova, S. Kotsilkov, E. Ivanov, N. K. Vitanov and R. Kotsilkova, Influence of polymer swelling and dissolution into food simulants on the release of graphene nanoplates and carbon nanotubes from poly (lactic) acid and polypropylene composite films, *J. Appl. Polym. Sci.*, 2017, **134**(44), 45469, DOI: 10.1002/app.45469.

44 C. Kirchkeszner, N. Petrovics, T. Tábi, N. Magyar, J. Kovács, B. S. Szabó, Z. Nyri and Z. Eke, Swelling as a promoter of migration of plastic additives in the interaction of fatty food simulants with polylactic acid-and poly-propylene-based plastics, *Food Control*, 2022, **132**, 108354, DOI: 10.1016/j.foodcont.2021.108354.

45 X. Hua, T. Zhang, Y. Duan, X. Liu, H. Wu, Y. Duan and J. Zhang, Hydrolytic degradation of PLA nanocomposites: impact of cellulose nanocrystal surface chemistry and dispersion state, *Cellulose*, 2025, **32**(14), 8135–8149, DOI: 10.1007/s10570-025-06717-2.

46 A. Moldovan, S. Cuc, D. Prodan, M. Rusu, D. Popa, A. C. Taut, I. Petean, D. Bombos, D. Rami and O. Nemes, Development and characterization of polylactic acid (PLA)-based nanocomposites used for food packaging, *Polymers*, 2023, **15**(13), 2855, DOI: 10.3390/polym15132855.

47 C. Da Porto, A. Natolino and D. Decorti, The combined extraction of polyphenols from grape marc: Ultrasound assisted extraction followed by supercritical CO2 extraction of ultrasound-raffinate, *LWT–Food Sci. Technol.*, 2015, **61**(1), 98–104, DOI: 10.1016/j.lwt.2014.11.027.

48 R. Re, N. Pellegrini, A. Proteggente, A. Pannala, M. Yang and C. Rice-Evans, Antioxidant activity applying an improved ABTS radical cation decolorization assay, *Free Radicals Biol. Med.*, 1999, **26**, 1231–1237.